Mathematisches Forschungsinstitut Oberwolfach

Report No. 8/2005

Mini-Workshop: Interface Problems in Computational Fluid Dynamics

Organised by
Eberhard Bänsch (Erlangen-Nürnberg)
Lutz Tobiska (Magdeburg)
Noel J. Walkington (Pittsburgh)

February 20th – February 26th, 2005

Abstract. Multiple difficulties are encountered when designing algorithms to simulate flows having free surfaces, embedded particles, or elastic containers. One difficulty common to all of these problems is that the associated interfaces are Lagrangian in character, while the fluid equations are naturally posed in the Eulerian frame. This workshop explores different approaches and algorithms developed to resolve these issues.

Mathematics Subject Classification (2000): 65M, 65N, 76.

Introduction by the Organisers

This workshop was concurrent with the workshop on Analytical and Numerical Methods in Image and Surface Processing (see: Report No. 10/2005), and since the participants interests overlapped several combined talks were organized. In particular, we thank P. Schroder, U. Reif, G. Dziuk, C. Elliot, and F. Cirak, for their contributions.

Currently there are three major techniques for tracking or characterizing interfaces present in a CFD computation: (i) The level set method, (ii) Phase field approximations, and (iii) Explicit parameterization using Lagrangian variables. Each of these techniques, and various hybrids, were presented by the participants to solve a variety of challenging CFD problems involving interfaces. Several trends emerged during the workshop.

(1) The analysis of phase field algorithms is much more advanced than that of the level set method (Elliot and Walkington).
(2) If the topology of the surface doesn't change, Lagrangian methods provide very accurate descriptions of the complex motions and physics of

the interfaces (see for example the Willmore flow by Dzuik). Many hybrid Eulerian/Lagrangian schemes were presented such as the immersed interface method (Gastaldi), volume of fluid method (Picasso), ALE and deforming mesh methods (Behr, Krahl, Mehnert, Ganesan).

The most detailed simulations presented at the workshop modeled hundreds of interacting rigid particles (Turek). The pistons and orientations of the particles were explicitly computed.

Progress has been made in the analysis of Lagrangian schemes to model interfacial motion (Dzuik, Mehnert, Nobile) for problems where the interface remains regular.

(3) Practical application of the level set technique appears to require frequent reparameterization of the level set function, and in order to obtain a sharp interface it is necessary to evaluate the Heavyside function of the level set function. These modifications to the basic algorithm represent a significant complication to the analysis of this class of methods. These complications also appear to extend to the practical implementation; for example, both Burman and Reusken evolve their interfaces using level sets, but explicitly construct a parametrization of the interface at each time step.

Mini-Workshop: Interface Problems in Computational Fluid Dynamics

Table of Contents

Abstracts

Free-surface Flow Modeling and Unstructured Space-time Meshes

Marek Behr

Free-surface flow simulations are an invaluable design and analysis tool in many areas of engineering, including civil engineering, marine and coating industries, and off-shore exploration. Two alternative computational approaches—interface-tracking and interface-capturing—are commonly considered. While the interface-capturing approach exhibits unmatched robustness for complex free-surface motion, i.e., merging and void formation, the interface-tracking approach is attractive due to its good mass conservation properties at low resolutions. Therefore, expanding the reach of the interface-tracking methods is of considerable interest. The fundamentals of our interface-tracking free-surface flow simulations—stabilized discretizations of Navier-Stokes equations, space-time formulations on moving grids, general mesh update mechanisms, and hydraulic structure applications—can be found in [1, 2] and references contained therein. In this report, we concentrate on an issue of temporally-refined graded space-time meshes.

In most space-time implementations to date, including the one used for the applications presented in this workshop, the meshes for the space-time slabs are simply extruded in the temporal direction from a spatial mesh, resulting in reference element domains that are always Cartesian products of spatial and temporal domains. Such an approach is best described as semi-unstructured (unstructured in space, structured in time) and does not leave the option of increasing temporal refinement in specific portions of the domain. In such case, the space-time slab exactly corresponds to a time step of a semi-discrete procedure.

Hughes and Hulbert [3] introduced the idea of adaptively-refined space-time mesh for a 1D elastic rod problem, and discussed the potential of unstructured space-time meshes as a more flexible and rigorous alternative to subcycling. Maubach [4] used unstructured space-time meshes to solve 1D parabolic problems. Idesman et al. [5] obtained the deformation history of a 2D viscoelastic plate by using an adaptively-refined space-time mesh. A similar approach was used by Sathe [6] to solve 2D parabolic problems. Yet, we are not aware of any tools that can currently provide a conformal unstructured space-time mesh covering complex domain for a 3D problem, which leads to a 4D space-time problem. We propose here a simple and robust procedure to generate 3D or 4D simplex-based space-time meshes.

Spatial Mesh As a starting point, we consider a spatial mesh in n_{sd} dimensions, generated using a standard 2D or 3D mesh generator. We restrict ourselves to n_{sd}-simplex-based meshes, i.e., triangular or tetrahedral.

Prism Formation Just like in traditional space-time implementation, the spatial mesh is at first extruded in the time dimension to fill the space-time slab contained

between time levels t_n and t_{n+1}. The extruded mesh is composed of prisms—6-noded space-time elements for 2D problems and 8-noded space-time elements for 3D problems. These elements, referred to as 3d6n and 4d8n, respectively, and illustrated in Figure 1(a), are the basis of the traditional space-time approach. Note that the "faces" extending in the temporal dimension are non-simplical, having 4 nodes for the 3d6n element, and 6 nodes for the 4d8n element. Our goal is to subdivide these prism-type elements into simplex-type elements 3d4n and 4d5n, shown in Figure 1(b).

(a) prism-type space-time elements (b) simplex-type space-time elements

FIGURE 1. Prism- and simplex-type space-time elements. Black and white nodes correspond to t_n and t_{n+1}, respectively.

Temporal Refinement The initial space-time mesh contains just two nodes for each of the nodes in the spatial mesh—e.g., in1 located at the bottom of the slab, and in2 located at the top, shown in Figure 2(a). The temporal refinement is accomplished by selectively adding one or more nodes along the line connecting the original nodes, as shown in Figure 2(b).

(a) original (b) refined

FIGURE 2. Temporal refinement of a 3d6n space-time prism.

Coordinate Perturbation The space-time faces of the prism-type elements will be subsequently divided into n_{sd}-simplices according to Delaunay criteria, *independently* for each prism. Since, at least for a non-moving spatial mesh, these faces are regular (rectangles for 2D and *right* prisms for 3D), the Delaunay mesh will not be unique. Therefore, there is no guarantee that the direction of diagonal line (2D) or diagonal triangle (3D) will be *compatible* across the neighboring space-time prisms (see Figure 3(a)). A simple solution is to randomly perturb the time-coordinates of some or all nodes, as illustrated in Figure 3(b). This perturbation, the same for each prism sharing a particular node, ensures the uniqueness of Delaunay process,

and guarantees compatibility of the n_{sd}-simplices between the neighboring space-time prisms. After the connectivity of the unstructured space-time mesh is established, the time-coordinates can be restored to their original values. In practice, the perturbation needs to be applied only to the space-time nodes corresponding to times greater than t_n.

(a) before (b) after

FIGURE 3. Perturbation of temporal coordinates of a `3d6n` prism.

Delaunay Triangulation The Delaunay method of generating simplex tessellations, although commonly used in 2D and 3D, is in principle applicable to any number of dimensions. Freely available implementations of the n-dimensional Delaunay algorithm are available, e.g., in the `qhull` [7] package. The Delaunay approach can be applied here without constraints or modifications because each space-time prism is *convex*.

Sliver Elimination The Delaunay approach, when applied to node sets where more than n_{sd} nodes may lie on a single plane (as is the case with non-simplical space-time prism faces), usually produces sliver simplices shown in Figure 4. Although the inner diagonal (marked `d1`) is unique due to the perturbation of time-coordinates, an additional element defined by both `d1` and `d2` may be also produced. An additional test is needed to detect and remove generated elements which have nearly-zero volume.

(a) sliver (b) final mesh

FIGURE 4. Sliver element elimination in a `3d6n` space-time prism.

Connectivity Generation Having constructed connectivity information inside each space-time prism, that a) incorporates new nodes placed between the slab-delimiting time levels, and b) is compatible between neighboring prisms, it is trivial to convert it into a global connectivity information, that connects all the space-time slab nodes in a network of $(n_{\mathrm{sd}}+1)$-simplex elements. Although this network is difficult to visualize in 4D, the computer program that generates it is largely

identical to the program that generates 3D space-time mesh from a 2D spatial mesh, which can be validated using available visualization tools. The proposed procedure has been applied to an externally-generated spatial triangular mesh around a cylinder, specifying higher levels of temporal refinement in the vicinity of the cylinder. Selected sections through the 3D space-time mesh so obtained are shown in Figure 5.

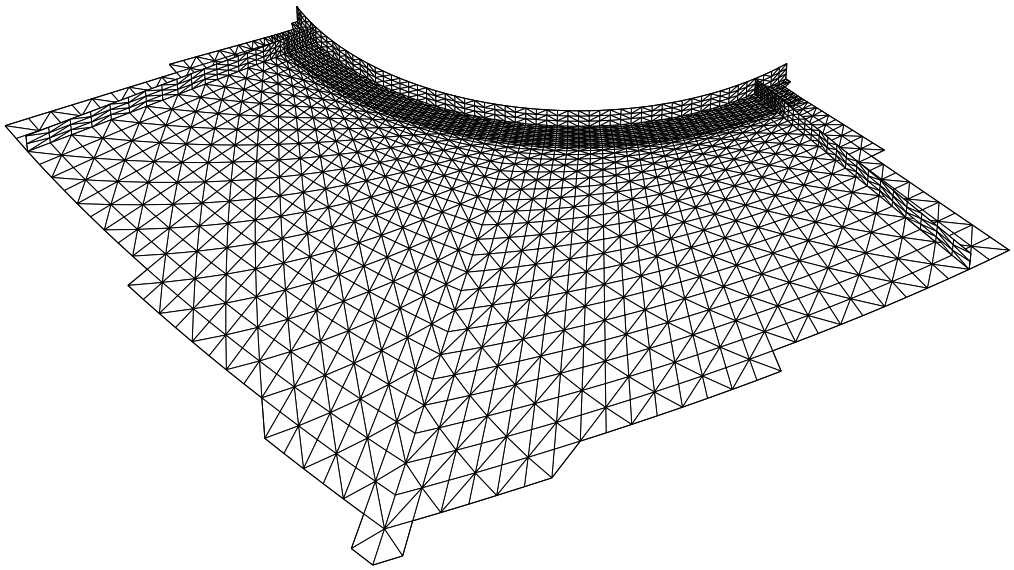

FIGURE 5. Portion of a temporally-refined 3D space-time mesh from 2D automatically-generated cylinder mesh.

Note that the same procedure is also applicable when the space-time mesh corresponds to a deforming domain. The simplices should be generated based on undeformed spatial mesh coordinates (assigning temporarily lower-level spatial coordinates to the upper-level and the temporal-refinement nodes). The technique does not extend however to situations where two different spatial meshes are to be connected with an unstructured space-time mesh.

REFERENCES

[1] M. Behr and F. Abraham, *Free Surface Flow Simulations in the Presence of Inclined Walls*, Computer Methods in Applied Mechanics and Engineering, **191** (2002), 5467–5483.

[2] M. Behr, *On the Application of Slip Boundary Condition on Curved Boundaries*, Intlernational Journal for Numerical Methods in Fluids **45** (2004), 43–51.

[3] T.J.R. Hughes and G.M. Hulbert, *Space-time finite element methods for elastodynamics: formulations and error estimates*, Computer Methods in Applied Mechanics and Engineering, **66** (1988), 339–363.

[4] J.M.L. Maubach, *Iterative Methods for Non-linear Partial Differential Equations*, Ph.D. thesis, University of Nijmegen, 1991.

[5] A. Idesman, R. Niekamp, and E. Stein, *Finite elements in space and time for generalized viscoelastic Maxwell model*, Computational Mechanics, **27** (2001), 49–60.

[6] S.V. Sathe, *Enhanced-Discretization and Solution Techniques in Flow Simulations and Parachute Fluid-Structure Interactions*, Ph.D. thesis, Rice University, Department of Mechanical Engineering and Materials Science, 2004.

[7] C.B. Barber, D.P. Dobkin, and H. Huhdanpaa, *The quickhull algorithm for convex hulls*, ACM Transactions on Mathematical Software, **22** (1996), 469–483.

A levelset finite element method for viscous free surface flow

Erik Burman
(joint work with Nicola Parolini)

In this communication we present some recent results on numerical procedures for finite element levelset methods for free surface flow. Three topics will be covered the first two of which represent joint work of the author with N. Parolini and is published in [Parolini, 2004].

- Stabilization of the level set advection equation,
- reinitialization procedures,
- discretization of Stokes problems with discontinuous coefficients.

We consider the case of unsteady incompressible flow of two immiscible Newtonian fluids. Let Ω be a domain divided in two subdomains Ω_1 and Ω_2 separated by an interface Γ. In each of the two subdomains Ω_i the flow is governed by the incompressible Navier–Stokes equations. To track the free surface we propose a levelset approach following [Dervieux and Thomasset, 1980] and [Sussman et al., 1994]. The evolution of the interface is obtained by solving an advection problem for a function ϕ such that $\phi < 0$ in one fluid and $\phi > 0$ in the other. The interface is given by the zero levelset of ϕ. The discontinuous physical quantities density, $\rho(\boldsymbol{x})$, and viscosity, $\mu(\boldsymbol{x})$, may then be derived from ϕ: $\rho(\boldsymbol{x}) = \mathrm{H}(\phi)\ \rho_1 + (1 - \mathrm{H}(\phi))\ \rho_2$, $\mu(\boldsymbol{x}) = \mathrm{H}(\phi)\ \mu_1 + (1 - \mathrm{H}(\phi))\ \mu_2$, where H denotes the Heaviside function. The Navier-Stokes equations are discretized with finite elements using the $P_1 isoP_2/P_1$ velocity/pressure pair. The advection equation is discretized on the $P_1 isoP_2$ space using a Galerkin method stabilized using subgrid viscosity.

Subgrid edge stabilization. In order to obtain a stable discretization of the advection equation with a minimal perturbation of the mass conservation properties of the Galerkin scheme we introduce a localized edge oriented stabilization. It was shown by Burman and Hansbo [Burman and Hansbo, 2003] that stabilization using penalization of the jumps in the gradient over all interior edges of the mesh yields a numerical scheme with optimal convergence properties for the transport equation. Another method for transport equations was proposed by Guermond in [Guermond, 1999] based on scale separation, so called subgrid viscosity. Here we introduce an operator penalizing the jump of the gradient over element edges only in the interior of the $P_1 isoP_2$ macro elements. Using a norm equivalence argument we show that the proposed operator can be cast in the framework given in [Guermond, 1999] and hence optimal a priori error estimates are obtained.

Reinitialization of the levelset function. The distance function property is not preserved under advection. In regions the level set function may become too flat leading to loss of accuracy in the interface location or too steep requiring

h	No reinit.	direct. reinit.	local proj. + HJ
0.1	0.65 %	8.56 %	0.80 %
0.05	0.15 %	3.03 %	0.17 %
0.025	0.05 %	1.06 %	0.06 %

TABLE 1. Relative mass loss for a rising bubble problem at $t = 0.1$, left without reinitialization, center using direct reinitialization, right using near field local projection and Hamilton-Jacobi

discontinuity capturing (high-resolution) schemes to suppress numerical oscillations. To counter these effects one wishes to *reinitialize* the distance function regularly. Given the interface position as a zero level set we reconstruct an approximate distance function in the finite element space. The approach we propose is based on a separation of the domain in the near field, consisting of the set of all elements containing the interface, and the far field. In the near field we use an exact local reinitialization on each element followed by a projection on the finite element space. In the far field any efficient reinitialization procedure is appropriate.

Given $\phi_{0,h}$ a piecewise linear levelset function defined on the interface subdomain $\Omega_{int} = \mathcal{T}_\Gamma = \left\{ \bigcup_{i=1}^{N} K_i : K_i \in \mathcal{T}, K_i \cap \Gamma \neq 0 \right\}$, an exact local reconstruction of the distance is given by:

$$d(\boldsymbol{x})|_{K_i} = \frac{\phi_{0,h}(\boldsymbol{x})}{|\nabla \phi_{0,h}|_{K_i}}, \quad K_i \in \mathcal{T}_\Gamma.$$

To get an approximation of the levelset function we project the discontinuous function $d(\boldsymbol{x})$ onto $V_h(\mathcal{T}_\Gamma)$

$$\int_{\mathcal{T}_\Gamma} \phi_h \, \psi_h \, dx = \int_{\mathcal{T}_\Gamma} d(\boldsymbol{x}) \, \psi_h \, dx \quad \forall \psi_h \in V_h(\mathcal{T}_\Gamma).$$

For this local reinitialization procedure we have proven optimal order convergence of the error in the $L^2(\Omega_{int})$-norm provided the interface is sufficiently smooth.

In the far field one may then use any efficient method for solving the eikonal equation such as the fast marching method or by solving a Hamilton-Jacobi equation. Numerical evidence shows that the proposed method is superior to some other methods proposed in literature as illustrated in Table 1.

An unfitted finite element method for Stokes' problem with discontinuous coefficients using Nitsche's method. It is well known that the solution of multifluid flow can not be expected to have better global regularity than $\mathbf{u} \in [H^1(\Omega)]^d$ and $p \in L^2_0(\Omega)$. This causes suboptimal convergence of any standard finite element method unless the mesh is fitted to the interface. However in case the interface is sufficiently regular, $\Gamma \in C^3$ and $dist(\Gamma, \partial\Omega) > 0$ one expects the solution to be more regular in each subdomain. Typically $\mathbf{u} \in [H^2(\Omega_1) \cup H^2(\Omega_2)]^d$ and $p \in H^1(\Omega_1) \cup H^1(\Omega_2)$. To exploit this property we introduce an unfitted finite element method inspired by [Hansbo and Hansbo, 2002] using techniques from

discontinuous Galerkin methods. Consider the following Stokes problem with discontinuous viscosity. For simplicity we here neglect surface tension effects

$$\begin{aligned} -2\mu_i \nabla \cdot \boldsymbol{\varepsilon}(u) + \nabla p &= f \quad \text{in } \Omega_i,\ i = 1,2 \\ \nabla \cdot u &= 0 \text{ in } \Omega \\ u &= 0 \quad \text{on } \partial\Omega, \end{aligned}$$

We introduce two conforming triangulations $\mathcal{T}_1$ and $\mathcal{T}_2$ such that, $\mathcal{T}_1 \cup \mathcal{T}_2 = \mathcal{T}_h(\Omega)$, $\mathcal{T}_1 \cap \mathcal{T}_2 = \mathcal{T}_\Gamma$ with the corresponding finite element spaces $V_h^i = \{v \in [C^0(\Omega_i)]^2 : v|_K \in [P^1(K)]^d, \forall K \in \mathcal{T}_i,\ v|_{\partial\Omega} = 0\}$, $Q_h^i = \{v \in L_0^2(\Omega_i) : v|_K \in P^0(K), \forall K \in \mathcal{T}_i\}$, with , $V_h = V_h^1 \cup V_h^2$, $Q_h = Q_h^1 \cup Q_h^2$. Let $[x]_e$ and $\{x\}_e$ denote the jump and the average of quantity x over edge e. We then propose the following finite element method: Find $(u_h, p_h) \in V_h \times Q_h$ such that

$$B[(u_h,p_h),(v_h,q_h)] + J_\Gamma((u_h,p_h),(v_h,q_h)) + J_p(p_h,q_h) = (f,v_h)_\Omega, \qquad \forall (v_h,q_h) \in V_h \times Q_h,$$

where $B[(u,p),(v,q)] = \sum_{i=1}^2 \Big((2\mu_i \boldsymbol{\varepsilon}(u), \boldsymbol{\varepsilon}(v))_{\Omega_i} - (p, \nabla\cdot v)_{\Omega_i} - (q, \nabla\cdot u)_{\Omega_i} \Big)$, $u_h|_{\Omega_i} = u_{h,i}$, $p_h|_{\Omega_i} = p_{h,i}$,

$$J_p(p_h,q_h) = \sum_{i=1,2} \sum_{K\in\mathcal{T}_i} \int_{\partial(K\cap\Omega_i)\setminus\partial\Omega_i} h\gamma_p [p_h][q_h] \, \mathrm{d}s.$$

The weak coupling takes the following form, if $\sigma(u_h,p_h)\cdot n = p_h n - 2\mu\boldsymbol{\varepsilon}(u_h)\cdot n$ then

$$\begin{aligned} J_\Gamma((u_h,p_h),(v_h,q_h)) = &\int_\Gamma \{\sigma(u_h,p_h)\cdot n\}[v_h] + \{\sigma(v_h,q_h)\cdot n\}[u_h] \, \mathrm{d}s \\ &+ \int_\Gamma \gamma\mu h^{-1}[u_h][v_h] \, \mathrm{d}s + \int_\Gamma \frac{\gamma_2}{2} h[\sigma(u_h,p_h)\cdot n]\cdot[\sigma(v_h,q_h)\cdot n] \, \mathrm{d}s \end{aligned}$$

For this formulation we prove a discrete inf-sup condition and optimal order error estimates in the triple norm including the H^1-norm of each subdomain and then in the L^2-norm using a duality argument.

References

[Burman and Hansbo, 2003] Burman, E. and Hansbo, P. (2003). Edge stabilization for Galerkin approximations of convection-diffusion problems. *Comput. Methods Appl. Mech. Engrg.*, 193:1437–1453.

[Dervieux and Thomasset, 1980] Dervieux and Thomasset (1980). *A finite element method for the simulation of Rayleigh-Taylor instability*, volume 771 of *Lecture Notes in Mathematics*. Springer-Verlag.

[Guermond, 1999] Guermond, J. L. (1999). Stabilization of galerkin approximation of transport equations by subgrid modeling. *M2AN Math. Model. Numer. Anal.*, 33:1293–1316.

[Hansbo and Hansbo, 2002] Hansbo, A. and Hansbo, P. (2002). An unfitted finite element method based on Nitsche's method for elliptic interface problems. *Computer Methods in Mechanics and Engineering*, 191(47–49):5537–5552.

[Parolini, 2004] Parolini, N. (2004). Computational fluid dynamics for naval engineering problems. Ecole Polytechnique Federale de Lausanne, These No 3138, 2004. `http://iacs.epfl.ch/~parolini/these_3138_Parolini.pdf`.

[Sussman et al., 1994] Sussman, M., Smereka, P., and Osher, S. (1994). A level set approach for computing solutions to incompressible two-phase flow. *J. Comp. Phys.*, 114:146–159.

Droplet Deformation with Navier Slip and Free Boundaries by Finite Elements

Sashikumaar Ganesan
(joint work with Lutz Tobiska)

For the numerical simulation of incompressible flows in fixed domains a large number of advanced approaches are available. The situation changes if the fluid domain is changing in time and the boundary or a part of it is a priori unknown and has to be determined during the solution process. In recent years some tools, like the ALE (Arbitrary Lagrangian Eulerian) method or the level set method have been used to capture the movement of free surfaces in time. These type of problems become more delicate if large deformations or surface tension effects have to be taken into account. It turns out that nowadays the development of robust and reliable algorithms for incompressible flows in moving domains is still a challenging problem.

As an example for an incompressible flow simulation in which large deformations and surface tension effects takes place we study the shape of a droplet impinging and spreading on a solid surface. The fluid flow in the droplet $\Omega(t) \subset \mathbf{R}^2$, $t \in [0, T]$ is governed by the incompressible Navier-Stokes equations

$$\frac{\partial \mathbf{u}}{\partial t} + (\mathbf{u} \cdot \nabla)\mathbf{u} - \nabla \cdot \sigma(\mathbf{u}, p) = \mathbf{f}, \qquad \nabla \cdot \mathbf{u} = 0, \qquad \text{in } \Omega(t),$$

the boundary conditions

$$\begin{aligned} \tau_F \cdot \sigma(\mathbf{u}, p)\nu_F = 0, \qquad \nu_F \cdot \sigma(\mathbf{u}, p)\nu_F = -\frac{\kappa}{\mathrm{We}} \qquad &\text{on } \Gamma_F(t) \\ \mathbf{u} \cdot \nu_S = 0, \qquad \tau_s \cdot \sigma(\mathbf{u}, p)\nu_s = -\beta \mathbf{u} \cdot \tau_s \qquad &\text{on } \Gamma_S(t) \end{aligned}$$

and the initial condition $\mathbf{u}(0) = (0, -1)$. Here $\mathbf{u} = (u_1, u_2)$ denotes the velocity, p the pressure, t the time, κ the curvature, $\mathbf{f} = (0, -Fr^{-1})$ the body force and

$$\sigma(\mathbf{u}, p) = \frac{1}{Re}(\nabla \mathbf{u} + \nabla \mathbf{u}^T) - p\mathbf{I}$$

the stress tensor. The Reynolds number Re, the Weber number We, and the Froude number Fr are the dimensionless parameter of the problem.

Note that $\beta \to \infty$ corresponds to the usual no-slip boundary condition, which leads to a singularity at the wetting points where the free-surface and solid-surface intersects. We prefer the Navier slip boundary condition because it is quite general [4, 5, 10] for these type of problems and by choosing an appropriate value for the slip coefficient β we can cover the whole range from applying almost no-slip up to the free-slip condition. In our numerical computations we have chosen a slip coefficient $\beta \geq 10^3$.

In the weak formulation of the problem, we replace the curvature term arising in the boundary integral over the free surface by the Laplace-Beltrami operator [1, 7]. Integration by part allows to avoid the calculation of second derivatives and to include a weak contact angle condition in the model. The time-dependent domain has been handled by the ALE approach [8] resulting in an additional convective term $(\mathbf{w} \cdot \nabla)\mathbf{u}$ in the Navier-Stokes equation where $\mathbf{w}$ is the domain velocity. We decompose the fluid domain into unstructured triangles and use the inf-sup stable pair of finite elements [3] consisting of piecewise quadratic functions enriched by cubic bubbles for the velocity components and piecewise linear discontinuous functions for the pressure. The strongly A-stable second order fractional step ϑ scheme [2, 9] has been used for the time discretization. In this time stepping scheme a semi-implicit form of curvature term has been applied. We then solve in each time step a Navier-Stokes problem for the velocity and pressure on a fixed domain and update the boundary as $\Gamma^{n+1} = \Gamma^n + \tau_n \mathbf{u}^{n+1}$. To find the displacements of the inner nodes within the new domain a linear elasticity equation is solved. Since the deformation of the domain is very large the mesh quality can be lost. To avoid this an automatic remeshing procedure has been used and the velocity and pressure fields are interpolated from the old domain.

The resulting algorithm has been implemented in the finite element package MooNMD [6]. In first numerical tests the influence of the impact velocity and the droplet diameter on the spreading length has been studied and compared with experimental results. In these calculations a mass loss of less than three percent has been observed.

This work was supported by Deutsche Forschungsgemeinschaft within in graduate program *Micro macro interactions in structured media and particle systems* (GK 828).

References

[1] E. Bänsch, *Finite element discretization of the Navier-Stokes equations with a free capillary surface*, Numer. Math., **88**, (2001), 203–235.

[2] M.O. Bristeau, R. Glowinski and J. Periaux, *Numerical methods for the Navier-Stokes equations. Application to the simulation of compressible and incompressible flows*, Comp. Phys. **6**, 1987, 73–188.

[3] M. Crouzeix and P.-A. Raviart, *Conforming and non conforming finite element methods for solving the stationary Stokes equation*, R.A.I.R.O. **R3**, 1973, 33–76.

[4] E.B. Dussan V, *The moving contact line: the slip boundary condition*, J. Fluid Mech., **77(4)**, 1976, 665–684.

[5] L.M. Hocking, *A moving fluid interface. Part 2. The removal of the force singularity by a slip flow* J. Fluid Mech. **79(2)**, 1977, 209–229.

[6] V. John and G. Matthies, *MooNMD - a program package based on mapped finite element methods*, Comput. Visual. Sci., **6**, 2004, 163–170.

[7] G. Matthies, *Finite element methods for free boundary value problems with capillary surfaces*, PhD thesis, Otto-von-Guericke-Universität Magdeburg, Fakultät für Mathematik, 2002.

[8] F. Nobile, *Numerical Approximation of Fluid-Structure Interaction Problems with Application to Haemodynamics*, PhD thesis, École Polytechnique Fédérale de Lausanne, 2001.

[9] S. Turek, *Efficient solvers for incompressible flow problems. An algorithmic and computational approach*, Springer-Verlag, Berlin, 1999.
[10] W.J. Silliman and L.E. Scriven, *Separating flow near static contact line: Slip at wall and shape of a free surface*, J. Comput. Phys., **34**, 1980, 287–313.

A finite element approach to the immersed boundary method

Lucia Gastaldi
(joint work with Daniele Boffi, Luca Heltai)

Fluid-structure interaction systems often involve the resolution of the fluid dynamic equations on a moving (that is, time dependent) domain. The immersed boundary method (IBM) was developed by Peskin (see [8, 9]) to study flow patterns around heart valves. The immersed boundary method is designed to handle a flexible boundary immersed in a fluid, hence it is particularly suited for biological fluid dynamic problems (see, e.g., [11, 7, 12, 6, 5]). The main idea of the method consists in considering the structure as a part of the fluid where additional forces are applied, and where additional mass may be localized. Therefore, instead of separating the system in its two components coupled by interface conditions, as it is conventionally done (see, e.g. [1, 10]), the incompressible Navier-Stokes equations, with a nonuniform mass density and an applied elastic force density, are used in order to describe the coupled motion of the hydroelastic system in a unified way. The advantage of this method is that the fluid domain can have a simple shape, so that structured grids can be used. On the other hand, the immersed boundary is typically not aligned with the grid and it is represented using Lagrangian variables, defined on a curvilinear mesh moving through the domain, independent of the fluid domain mesh.

For the sake of simplicity, we consider the model problem of a viscous incompressible fluid in a two-dimensional square domain Ω containing an immersed massless elastic boundary in the form of a curve. We refer the interested reader to [4] for a review of other applications.

To be more precise, for all $t \in [0,T]$, let Γ_t be a simple closed curve, the configuration of which is given in a parametric form, $\mathbf{X}(s,t)$, $0 \le s \le L$, $\mathbf{X}(0,t) = \mathbf{X}(L,t)$. The equations of motion of the system are

$$\rho\frac{\partial \mathbf{u}}{\partial t} - \mu\Delta\mathbf{u} + \mathbf{u}\cdot\boldsymbol{\nabla}\,\mathbf{u} + \boldsymbol{\nabla}\,p = \mathbf{F} \quad \text{in } \Omega\times\,]0,T[\tag{1}$$

$$\nabla\cdot\,\mathbf{u} = 0 \quad \text{in } \Omega\times\,]0,T[\tag{2}$$

$$\mathbf{F}(\mathbf{x},t) = \int_0^L \kappa\frac{\partial^2\mathbf{X}(s,t)}{\partial s^2}\delta(\mathbf{x}-\mathbf{X}(s,t))\,ds \quad \forall\mathbf{x}\in\Omega,\ t\in\,]0,T[\tag{3}$$

$$\frac{\partial\mathbf{X}}{\partial t}(s,t) = \mathbf{u}(\mathbf{X}(s,t),t) \quad \forall s\in[0,L],\ t\in\,]0,T[\tag{4}$$

Here $\mathbf{u}$ is the fluid velocity and p is the fluid pressure. The problem is completely described once we fix boundary and initial conditions:

$$\mathbf{u} = 0 \qquad \text{on } \partial\Omega \times]0,T[\tag{5}$$

$$\mathbf{u}(\cdot,0) = \mathbf{u}_0(\cdot) \qquad \text{on } \Omega \tag{6}$$

$$\mathbf{X}(s,0) = \mathbf{X}_0(s) \qquad \forall s \in [0,L]. \tag{7}$$

We observe that the choice of $\mathbf{F}$ is made in such a way that the motion of the boundary $\mathbf{X}$ is driven by its elastic energy (κ denotes the elasticity coefficient). The main mathematical result that allows us to deal, in a variational way, with the approximation of the Dirac mass appearing in (3), is the following lemma.

Lemma 1. *Assume that, for all $t \in [0,T]$, the immersed boundary Γ_t is Lipschitz continuous. Assume, moreover, that $\mathbf{X}$ is regular enough so that the right hand side of (8) makes sense. Then for all $t \in]0,T[$, the force density $\mathbf{F}(t)$, defined formally in (3), is a distribution function belonging to $H^{-1}(\Omega)^2$ defined as follows: for all $\mathbf{v} \in H_0^1(\Omega)$*

$$ {}_{H^{-1}}\!<\mathbf{F}(t),\mathbf{v}>_{H_0^1} = \int_0^L \kappa \frac{\partial^2 \mathbf{X}(s,t)}{\partial s^2} \cdot \mathbf{v}(\mathbf{X}(s,t))\, ds \quad \forall t \in [0,T]. \tag{8}$$

Lemma 1 allows to write the Navier-Stokes equations in their variational form which is well suited to the finite element discretization. The well-posedness of the problem composed by the variational form of the Navier-Stokes equations together with (8), (4), (5), (6) and (7) has been discussed in [2] for a one dimensional model.

The original numerical approach to the IBM is based on finite differences for the spatial discretization. This employs two independent grids, one for the Eulerian variables in the fluid and the other for the Lagrangian variables associated with the immersed boundary. The main difficulty in such spatial discretization consists in the construction of a suitable regularization of the Dirac delta function which is used to take into account the interaction equations, see [9]. Our approach to the discretization of the IBM is completely based upon the finite element method. Thanks to Lemma 1, we deal with the Dirac delta function, which is related to the forces exerted by the immersed structure on the fluid and viceversa, in a variational way. So that there is no need to construct a regularization of the delta function, but its effect is taken into account by its action on the test functions.

Let us consider discrete space sequences $\mathbf{V}_h \subset H_0^1(\Omega)^d$ and $Q_h \subset L_0^2(\Omega)$ which provide a stable approximation of the Stokes equations. The approximation of the immersed curve is obtained by piecewise linear continuous vector valued functions $\mathbf{S}_h$. For the sake of simplicity we discard the nonlinear term in the Navier–Stokes equations; numerical results for the fully nonlinear system are in progress. Then we consider the following discrete problem: given $\mathbf{u}_{0h} \in \mathbf{V}_h$ and $\mathbf{X}_{h\,0} \in \mathbf{S}_h$, for all $t \in]0,T[$, find $(\mathbf{u}_h(t), p_h(t)) \in \mathbf{V}_h \times Q_h$ and $\mathbf{X}_h(t) \in \mathbf{S}_h$, such that

$$\rho \frac{d}{dt}(\mathbf{u}_h(t),\mathbf{v}) + \mu(\boldsymbol{\nabla}\,\mathbf{u}_h(t), \boldsymbol{\nabla}\,\mathbf{v}) - (\nabla\cdot\mathbf{v}, p_h(t)) = <\mathbf{F}_h(t),\mathbf{v}> \quad \forall \mathbf{v} \in \mathbf{V}_h \tag{9}$$

$$(\nabla\cdot\mathbf{u}_h(t), q) = 0 \qquad \forall q \in Q_h \tag{10}$$

with

$$(11) \qquad < \mathbf{F}_h(t), \mathbf{v} >= \sum_{i=0}^{m-1} \kappa \left(\frac{\partial \mathbf{X}_{h\,i+1}}{\partial s}(t) - \frac{\partial \mathbf{X}_{h\,i}}{\partial s}(t) \right) \mathbf{v}(\mathbf{X}_{h\,i}(t)) \qquad \forall \mathbf{v} \in \mathbf{V}_h$$

$$(12) \qquad \frac{\partial \mathbf{X}_{h\,i}}{\partial t}(t) = \mathbf{u}_h(\mathbf{X}_{h\,i}(t), t) \qquad \forall i = 0, 1, \cdots, m$$

$$(13) \qquad \mathbf{u}_h(\mathbf{x}, 0) = \mathbf{u}_{0h}(\mathbf{x}) \ \forall \mathbf{x} \in \Omega \qquad \mathbf{X}_{h\,i}(0) = \mathbf{X}_0(s_i) \ \forall i = 1, \cdots, m.$$

The following stability property for the solution of this problem holds true:

$$(14) \qquad \frac{1}{2}\frac{d}{dt}||\mathbf{u}_h(t)||_0^2 + \mu||\,\mathbf{grad}\,\mathbf{u}_h(t)||_0^2 + \frac{\kappa}{2}\frac{d}{dt}\left\|\frac{\partial \mathbf{X}_h(t)}{\partial s}\right\|_0^2 \leq 0.$$

The time discretization is based on the backward Euler method. In our problem, the Navier-Stokes equations (9)-(10) are strongly coupled through the source term (8) with the system of ordinary differential equations given by (12). Therefore, in order to avoid the resolution of a fully nonlinear system of equations at each time step, we adopt a natural modification of the backward Euler method. Then, our scheme consists of two steps: given the approximation $\mathbf{X}_h^n$ of $\mathbf{X}$ at time $n\Delta t$, we construct $\mathbf{F}_h^{n+1}$ and find the solution $(\mathbf{u}_h^{n+1}, p_h^{n+1})$ to the Navier-Stokes equations; then we move the immersed boundary, getting $\mathbf{X}_h^{n+1}$. A conditioned stability property can also be proved for the full time-space discretization.

We refer the interested reader to [2, 3, 4] for the derivation of our numerical schemes and for several experimental results confirming the robustness of the scheme.

References

[1] K.J. Bathe, H. Zhang, and S. Ji, *Finite element analysis of fluid flows fully coupled with structural interactions*, Computers & Structures **72** (1999), 1-16.

[2] D. Boffi, and L. Gastaldi *A finite element approach for the immersed boundary method*, Computers & Structures **81** (2003), 491-501.

[3] D. Boffi and L. Gastaldi, *The immersed boundary method: a finite element approach*, Proc. of the Second M.I.T. Conference on Computational Fluid and Solid Mechanics (K.J. Bathe, ed.), vol. 2, Elsevier, (2003) 1263-1266.

[4] D. Boffi, L. Gastaldi, and L. Heltai, *A finite element approach to the immersed boundary method*, Progress in Engineering Computational Technology, B.H.V. Topping and C.A. Mota Soares Eds., Saxe-Coburg Publications, Stirling, Scotland, **Chapt. 12** (2004), 271-298.

[5] L.J. Fauci and C.S. Peskin, *A computational model of aquatic animal locomotion*, J. Comput. Phys. **77** (1988), 85-108.

[6] E. Givelberg, *Modeling elastic shells immersed in fluid*, Comm. Pure Appl. Math. **57** (2004), 283-309.

[7] C.S. Peskin and D.M. McQueen *Computational biofluid dynamics*, Fluid dynamics in biology (Seattle, WA, 1991), Contemp. Math., vol. 141, Amer. Math. Soc., Providence, RI, (1993), 161-186.

[8] C.S. Peskin *Numerical analysis of blood flow in the heart*, J. Computational Phys. **25** (1977), 220-252.

[9] C.S. Peskin *The immersed boundary method*, Acta Numerica 2002, Cambridge University Press, (2002), 1-39.

[10] A. Quarteroni, *Modeling the cardiovascular system: a mathematical challenge*, Mathematics Unlimited – 2001 and Beyond, (B. Engquist and W. Schmid, eds.), Springer-Verlag, (2001), 961-972.
[11] M. E. Rosar and C. S. Peskin *Fluid flow in collapsible elastic tubes: a three-dimensional numerical model*, New York J. Math., **7**, (2001), 281-302.
[12] L. Zhu and C.S. Peskin *Simulation of a flapping flexible filament in a flowing soap film by the immersed boundary method*, J. Comput. Phys. **179** (2002), 452-468.

Numerical Investigation of the Non-Isothermal Contact Angle

Rolf Krahl
(joint work with Eberhard Bänsch)

1. Introduction

It is known from experiments that thermal effects have a considerable impact on the shape of a gas–liquid phase boundary and on the contact angle at it meets a solid wall. Gerstmann et al. investigated in [5] the reorientation of a gas–liquid phase boundary upon step reduction of gravity in the non-isothermal case. In this scenario of a cold liquid meniscus spreading over a hot solid wall, the contact angle was observed to become larger then in the isothermal case. In order to investigate this phenomenon numerically, we focus on the effect of Marangoni convection on the shape of the phase boundary. Therefore, we limit ourselves to the case where no external body forces act on the fluid.

2. Numerical setup

Consider a circular cylinder, partly filled with liquid (see Fig. 1). We assume to have no gravity. In the isothermal case, the shape of the gas–liquid phase boundary will be spherical if the liquid is at rest. Now we assume the cylinder wall to be split in two parts: the lower part and the bottom Γ_C is cold, while the upper part Γ_H is heated. The gas–liquid phase boundary Γ_S is assumed to be adiabatic. The liquid is cold initially.

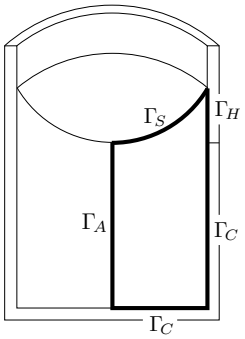

Figure 1. Computational domain

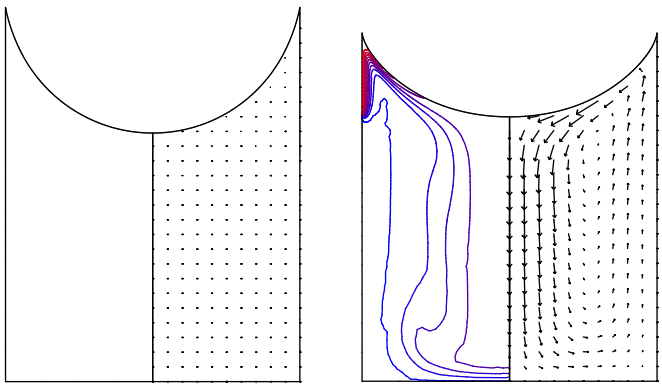

FIGURE 2. Shape of the free surface, isolines of temperature and velocity field in the in the isothermal case (left) and in the case of Marangoni convection (right).

The flow field in the liquid is governed by the incompressible Navier–Stokes equations. We assume no-slip boundary conditions at the cylinder wall. At the phase boundary the stress is prescribed. The free surface moves with the normal component of the velocity. A static contact angle is imposed as a boundary condition for the surface. For the heat transport, an advection-diffusion equation has to be solved.

3. Numerical methods

A finite element method is used to solve the numerical problem. The structure of the solver and the time discretization scheme is described in [1].

Key ingredient of the method for incorporating surface tension effects is the proper treatment of the free capillary boundary. To this end, a variational formulation for the curvature terms yields an accurate, dimensionally-independent and simple-to-implement approximation. The solver uses a stable time discretization, that is semi-implicit with respect to the treatment of the curvature terms. This firstly allows one to choose the time step independently of the mesh size—as opposed to common "explicit" treatments of the curvature terms—and secondly decouples the computation of the geometry and the flow field. This approach has proven to be both efficient and robust. For details see [2].

Applications of this method to some practical flow problems can be found for instance in [2, 3, 4].

4. Results

In the non-isothermal case, a temperature gradient induces a Marangoni stress at the phase boundary, exciting a flow in the liquid and a deformation of the free surface (Fig. 2). The shape of the non-isothermal phase boundary is significantly flattened near the center compared to the isothermal reference configuration (Fig. 3, left). The tangent to the surface at some given point meets the cylinder wall with an higher angle then in the isothermal case (Fig. 3, center). While the curvature of

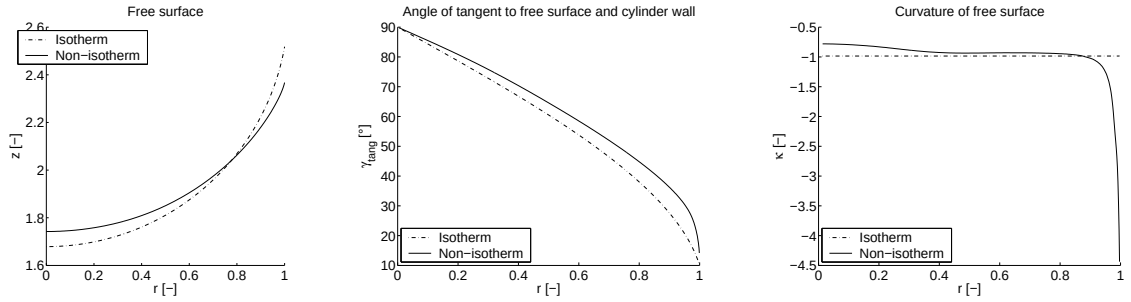

FIGURE 3. Shape of the free surface (left). Angle of the tangent to the free surface and the vertical cylinder wall (center). Curvature of the free surface (right).

the free surface is constant in the isothermal configuration, in the non-isothermal case it is much larger near the cylinder wall then in the center (Fig. 3, right). One might assume that this strong variation in curvature within a small layer close to the wall is hardly visible to the eye. This could explain why the contact angle in the non-isothermal configuration *appears* to be larger then in the isothermal case, although it was prescribed as a boundary condition with the same value in both cases.

REFERENCES

[1] E. Bänsch. *Simulation of instationary, incompressible flows*. Acta Math. Univ. Comenianae, 67(1), pp. 101–114, 1998.

[2] E. Bänsch. *Finite element discretization of the Navier–Stokes equations with free capillary surface*. Numer. Math., 88(2), pp. 203–235, 2001.

[3] E. Bänsch, C. P. Berg, and A. Ohlhoff. *Uniaxial, extensional flows in liquid bridges*. J. Fluid Mech., 521, pp. 353–379, 2004.

[4] E. Bänsch and B. Höhn. *Numerical simulation of a silicon floating zone with a free capillary surface*. In F. Keil, W. Mackens, H. Vo, and J. Werther, eds., Scientific computing in chemical engineering II, Springer, 1999, volume 1, pp. 328–335.

[5] J. Gerstmann, M. Michaelis, and M. E. Dreyer. *Capillary driven oscillations of a free liquid interface under non-isothermal conditions*. Proc. Appl. Math. Mech., 4(1), pp. 436–437, 2004.

[6] R. Krahl and E. Bänsch. *Impact of marangoni effects on the* apparent *contact angle — a numerical investigation*. To appear in Microgravity – Science and Technology.

Numerical simulation of the Rosensweig instability of ferrofluids in the static and dynamic case

GUNAR MATTHIES

(joint work with Olga Lavrova, Lutz Tobiska)

If a uniform magnetic field is applied perpendicular to a layer of a ferrofluid then a spontaneous surface deformation occurs provided the field strength exceeds a critical value. This behaviour is called Rosensweig instability and was first observed

by Cowley and Rosensweig [2]. It is caused by the interaction of gravitational, capillary and magnetic forces. Additionally, in the transition from the undisturbed surface to the fully developed pattern, hydrodynamic forces have to be taken into consideration. Stability analysis of this phenomenon is often restricted to determine the critical magnetic field intensity in the case of small perturbations [5].

Our numerical simulation is based on the nonlinear system of coupled Maxwell and Navier-Stokes equations together with the Young-Laplace equation, representing the force balance at the unknown free surface. We describe numerical algorithms to handle both the static and the dynamic case. Simplified numerical models for the static case have been already studied in [1, 3].

The Maxwell equations for a nonconducting fluid are given by

$$\operatorname{curl} \mathbf{H} = \mathbf{0}, \quad \operatorname{div} \mathbf{B} = 0 \qquad \text{in } \Omega$$

with the magnetic field strength $\mathbf{H}$ and the magnetic induction $\mathbf{B}$ satisfying the constitutive relation

$$\mathbf{B} = \begin{cases} \mu_0(\mathbf{M} + \mathbf{H}) & \text{in } \Omega_F(t) \\ \mu_0 \mathbf{H} & \text{in } \Omega \setminus \Omega_F(t) \end{cases}$$

where $\mathbf{M}$ is the magnetisation, $\mu_0 = 4\pi \cdot 10^{-7}\mathrm{Vs/Am}$ is the permeability constant, $\Omega_F(t)$ is the subdomain occupied by the ferrofluid at time t. The magnetisation $\mathbf{M}$ is assumed to be parallel to the magnetic field $\mathbf{H}$ and to follow the Langevin law, i.e.,

$$M = M_S \left(\coth(\gamma|\mathbf{H}|) - \frac{1}{\gamma|\mathbf{H}|} \right) \frac{\mathbf{H}}{|\mathbf{H}|}$$

with the saturation magnetisation M_S, the Langevin parameter $\gamma = 3\chi_0/M_S$, and the initial susceptibility χ_0. The hydrodynamical properties are described by the time-dependent incompressible Navier-Stokes equations

$$\begin{aligned} \varrho(\mathbf{u}_t + (\mathbf{u} \cdot \nabla)\mathbf{u} = \operatorname{div} \sigma(u, p, H) + f \qquad & \text{in } \Omega_F(t),\ t > 0, \\ \operatorname{div}\, u = 0 \qquad & \text{in } \Omega_F(t),\ t > 0 \end{aligned}$$

where $\sigma(u, p, H)$ is the stress tensor with

$$\sigma_{ij} = \eta \left(\frac{\partial u_i}{\partial x_j} \frac{\partial u_j}{\partial x_i} \right) - \left(p - \frac{\mu_0}{2} |\mathbf{H}|^2 \right) \delta_{ij} + B_i H_j, \qquad i, j = 1, 2, 3.$$

Here, ϱ denotes the density, η the dynamic viscosity, $\mathbf{u}$ the velocity, and p the pressure. Finally, we have the force balance at the free surface and the kinematic condition

$$[|\sigma \mathbf{n}|] = \alpha \mathcal{K} \mathbf{n}, \qquad \mathbf{u} \cdot \mathbf{n} = V_\Gamma \qquad \text{on } \Gamma_F(t),\ t > 0$$

with the sum of the principal curvatures $\mathcal{K}$, the coefficient of surface tension α, the unit normal vector $\mathbf{n}$, the normal velocity V_Γ of the free surface Γ_F.

The coupled problem is iteratively splitted into subproblems which depend on whether the static or dynamic case is considered. In the static case we have $\mathbf{u} = \mathbf{0}$ and the pressure p can be determined directly from the Navier-Stokes equations. Thus, in this case we solve a 3D magnetostatic problem inside and outside of the

fluid for a given Ω_F and update Ω_F by solving the 2D Young-Laplace equation for the graph representing Γ_F. In the dynamic case we incorporate the force balance on $\Gamma_F(t)$, i.e. the Young-Laplace equation, in the flow calculation which leads to the following iteration: Given $\Omega_F(t_n)$ we solve a 3D magnetostatic problem inside and outside of the fluid, a 3D Navier-Stokes problem in a time-dependent domain by the ALE (Arbitrary Lagrangian Eulerian) method, and use the information $\mathbf{u} \cdot \mathbf{n}$ at $\Gamma_F(t_n)$ to find the position for $\Gamma_F(t_{n+1})$.

For approximating the solutions finite element methods were applied. The nonlinear subproblems were solved by a fixed-point iteration and the arising linear systems of equations by multi-level algorithms, [4].

While theoretical results are available for the subproblems, like the Navier-Stokes equations in a fixed domain, the magnetostatic problem and the Young-Laplace equation, the mathematical analysis of the fully coupled problem is still an ongoing challenge.

The numerical simulations show in both cases that accurate finite element solutions for the peak shapes and heights can be obtained. Moreover, the critical magnetic field for the onset of instability can be determined accurately. Damped oscillations converging into the stationary limit can be observed if a supercritical field is switched on suddenly.

This work was partly supported by the German Research Foundation (DFG-FOR 301) and the State Sachsen-Anhalt.

References

[1] V.G. Bashtovoi, O.A. Lavrova, V.K. Polevikov, L. Tobiska, *Computer modeling of the instability of a horizontal magnetic fluid layer in a uniform magnetic field*, JMMM **252** (2002), 299-301.

[2] M.D. Cowley, R.E. Rosensweig, *The interfacial stability of a ferromagnetic fluid*, J.Fluid Mech. **30** (1967), 671-688.

[3] O.A. Lavrova, G. Matthies, T. Mitkova, V.K. Polevikov, L. Tobiska, *Finite element methods or coupled problems in ferrohydrodynamics*, in: Challenges in Scientific Computing CISC 2002, ed. by E. Bänsch, Lect. Notes Comp. Sci. Engrg. 35, Springer-Verlag, 2003, 160-183.

[4] G. Matthies, *Finite element methods for free boundary value problems with capillary surfaces*, Ph.D thesis, Fakultät für Mathematik, Otto-von-Guericke-Universität Magdeburg, 2002, published at Shaker-Verlag Aachen.

[5] R.E. Rosensweig, *Ferrohydrodynamics*, Dover Publ., Mineola, New York, 1997.

Convergence of a semidiscrete scheme for a model problem with a capillary boundary condition

Jürgen Mehnert

We may think of a fluid in a container occupying the time dependent two dimensional domain $\Omega(t)$ with a free boundary $\Gamma(t)$ assumed to be a graph. The rigid bottom of the container is denoted by Γ_D. To avoid problems concerning contact angles we consider periodic lateral boundary conditions.

In general the motion of a fluid with a free boundary is described by the Navier–Stokes equations with a capillary boundary condition. Let us focus on the problems arising from the curvature in the capillary boundary condition caused by the surface tension. At the same time we want to neglect the difficulties which are due to the divergence free condition. Therefore, we simplify the Navier–Stokes equations in order to obtain a model problem.

Thus, we are led to the following model problem. Find the time dependent domain $\Omega(t)$ and the field variable $u(\cdot,t) : \Omega(t) \to \mathbb{R}^2$ such that

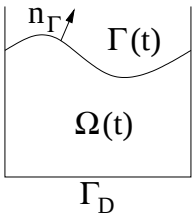

$$\begin{aligned} u_t - \Delta u &= f && \text{in } \Omega(t) \\ \partial u/\partial \nu &= \kappa\,\nu && \text{on } \Gamma(t) \\ v &= u \cdot \nu && \text{on } \Gamma(t) \\ u &= 0 && \text{on } \Gamma_D \\ u(0) &= u_0 && \text{in } \Omega_0\,, \end{aligned}$$

where u_0 denotes the initial value of u and Ω_0 the initial domain. Moreover, ν is the outer unit normal to the free boundary $\Gamma(t)$, κ its curvature and v its normal velocity. The external forces are denoted by f.

Following the same line as in [1] we introduce a semidiscrete scheme for the model problem based on a finite element approximation using piecewise linear functions and prove an optimal a priori error estimate for the field variable and the free boundary, see [6].

There is only one previous paper concerning error estimates for this kind of problems we are aware of. In [7] a stationary model free boundary problem is introduced and an error estimate for the field variable and the free boundary is proved. Unfortunately, there seems to be no possibility to extend these methods to the instationary case.

The key idea in deriving our error estimate is to work with the geometric quantities of the problem. This idea is due to Deckelnick and Dziuk and was introduced in [3], where error estimates for the mean curvature flow were proved. In the meanwhile this technique was also applied to surface diffusion, see [2] and [5], and to Willmore flow, see [4].

To extend the underlying method to the Navier–Stokes equations with a free capillary boundary one needs an appropriate approximation of u which should be divergence free and has the required approximation properties. In [8] such an operator is introduced for the stationary problem.

References

[1] E. Bänsch, *Finite element discretization of the Navier–Stokes equations with a free capillary surface,* Numer. Math., 88 (2001), pp. 203–235.

[2] E. Bänsch, P. Morin, R.H. Nochetto, *Surface Diffusion of Graphs: Variational Formulation, Error Analysis and Simulation,* SIAM J. Numer. Anal., 42 (2004), pp. 773–799.

[3] K. Deckelnick, G. Dziuk, *Error estimates for a semi–implicit fully discrete finite element scheme for the mean curvature flow of graphs,* Interfaces Free Bound., 2 (2000), pp. 341–359.

[4] K. Deckelnick, G. Dziuk, *Error estimates for the Willmore flow of graphs,* Preprint Universität Freiburg, Nr. 25/04, (2004).
[5] K. Deckelnick, G. Dziuk, C.M. Elliott, *Error analysis of a semidiscrete numerical scheme for diffusion in axially symmetric surfaces,* SIAM J. Numer. Anal., 41 (2003), pp. 2161–2179.
[6] J. Mehnert, *Konvergenz eines semidiskreten Verfahrens zu einem Modellproblem mit Kapillarrandbedingung,* PhD–thesis, Universität Freiburg, (2004).
`www.freidok.uni-freiburg.de/volltexte/1562/`
[7] P. Saavedra, L.R. Scott, *Variational Formulation of a Model Free–Boundary Problem,* Math. Comp., 57 (1991), pp. 451–475.
[8] M. Tabata, D. Tagami, *A finite element analysis of a linearized problem of the Navier–Stokes equations with surface tension,* SIAM J. Numer. Anal., 38 (2000), pp. 40–57.

Added mass effect in the design of partitioned fluid structure algorithms

Fabio Nobile
(joint work with Paola Cusin, Jean Frédéric Gerbeau)

We are interested in simulating the mechanical interaction between blood and arterial wall. Typical geometries appearing in this application have a cylindrical structure. Large arteries feature deformations up to 10% of the diameter, hence relatively large deformations of the domain have to be accounted for in simulations. We suppose the fluid to be Newtonian and we model it by the incompressible Navier-Stokes equations in Arbitrary Lagrangian Eulerian formulation. The structure is described either by a 1D generalized string model [4] (for 2D simulations) or by a nonlinear shell model in large displacements regime (for 3D simulations). The coupling conditions enforce the continuity of velocities and stresses at the interface between fluid and structure.

To simulate the interaction we focus on partitioned time marching algorithms, that is, algorithms which solve sequentially the fluid and the structure subproblems, thus allowing one to reuse existing computational codes. They can be of explicit or implicit type: in the former case, the fluid and structure subproblems are solved only once (or just few times) within each time step, yet they do not ensure exact balance of energy. In the latter case, conversely, a good energy balance is achieved, yet at the price to solve a non-linear problem at each time step, often demanding several subiterations between fluid and structure.

In our experience, explicit algorithms become unstable, irrespectively of the time discretization parameter employed, under certain combinations of physical parameters. In particular this occurs when the density of the structure becomes too small with respect to the density of the fluid or when the aspect ratio of the computational domain (length of the artery compared to its diameter) becomes too large.

The aim of this work is to give a mathematical explanation of such phenomena, by analyzing a simplified fluid structure model. More precisely, we consider the coupling between an axisymmetric potential flow with a thin elastic tube deforming only in the radial direction . Let $\Omega = \{(z,r) \in \mathbb{R}^2,\ 0 < z < L,\ 0 < r < R\}$ be

the 2D axisymmetric fluid domain and $\Sigma = \bar{\Omega} \cap \{r = R\}$ the interface with the structure. Denoting by $(\mathbf{u}, p)$ the fluid velocity and pressure and by η the structure radial deformation, we consider the coupled problem

$$\begin{cases} \rho_f \partial_t \mathbf{u} + \nabla p = 0 & \text{in } \Omega \\ \operatorname{div} \mathbf{u} = 0 & \text{in } \Omega \\ \rho_s h_s \partial_{tt}^2 \eta + a\eta = p & \text{on } \Sigma \\ \mathbf{u} \cdot \mathbf{n} = \partial_t \eta & \text{on } \Sigma. \end{cases} \tag{1}$$

Here, ρ_f and ρ_s are the fluid and structure densities, respectively, a an elastic coefficient and h_s the structure thickness.

The fluid and structure subproblems have to be supplemented with initial conditions and further boundary conditions on the remaining portions of the boundary. In particular, on the "inflow" section ($\Gamma_{in} = \bar{\Omega} \cap \{z = 0\}$) and "outflow" section ($\Gamma_{out} = \bar{\Omega} \cap \{z = L\}$) we prescribe a given pressure $\bar{p} = \bar{p}(t, z, r)$.

The fluid equations can be rewritten in terms of the pressure only as

$$\begin{cases} \triangle p = 0 & \text{in } \Omega \\ \partial_{\mathbf{n}} p = -\rho_f \partial_{tt}^2 \eta & \text{on } \Sigma \\ p = \bar{p} & \text{on } \Gamma_{in} \cap \Gamma_{out} \end{cases} \tag{2}$$

We introduce, now, the *added-mass operator* $\mathcal{M}_A : H^{-1/2}(\Sigma) \to H^{1/2}(\Sigma)$ as

$$\forall \xi \in H^{-1/2}(\Sigma) \qquad \mathcal{M}_A \xi = w|_\Sigma, \quad \text{where } \begin{cases} \triangle w = 0 & \text{in } \Omega \\ w = 0 & \text{on } \Gamma_{in} \cup \Gamma_{out} \\ \partial_n w = \xi & \text{on } \Sigma \end{cases}$$

The operator $\mathcal{M}_A$ is the inverse of the standard Steklov-Poincarée operator and is compact, self-adjoint and positive in $L^2(\Sigma)$. In particular, for a cylindrical geometry, its maximum eigenvalue μ_{max} depends on the aspect ratio L/R of the domain and asymptotically for $L/R \to \infty$ is given by $\mu_{max} \approx 2L^2/(\pi^2 R)$. With the aid of the added-mass operator, the fluid-structure problems (1) can be rewritten as a modified structure problem:

$$(\rho_s h_s \mathcal{I} + \rho_f \mathcal{M}_A)\partial_{tt}^2 \eta + a\eta = p_{ext} \quad \text{on } \Sigma, \tag{3}$$

where $\mathcal{I}$ is the identity operator and p_{ext} accounts for the non homogeneous boundary conditions on Γ_{in} and Γ_{out}. In this model, the presence of the fluid appears as an extra mass on the structure.

Model (3) (respectively (1)) being linear, it can be used to investigate the stability of partitioned fluid-structure algorithms. As a prototype of an *explicit* time marching scheme we consider the one obtained by discretizing the structure equation in (1) with a leap-frog (explicit) scheme and the fluid part with the

implicit Euler scheme :

$$
(4)\qquad \begin{cases} \rho_f \dfrac{\mathbf{u}^n - \mathbf{u}^{n-1}}{\Delta t} + \nabla p^n = 0 & \text{in } \Omega \\ \operatorname{div} \mathbf{u}^n = 0 & \text{in } \Omega \\ \rho_s h_s \dfrac{\eta^{n+1} - 2\eta^n + \eta^{n-1}}{\Delta t^2} + a\eta^n = p^n & \text{on } \Sigma \\ \mathbf{u}^n \cdot \mathbf{n} = \dfrac{\eta^n - \eta^{n-1}}{\Delta t} & \text{on } \Sigma. \end{cases}
$$

In [3] it is shown that this time discretization scheme becomes *unconditionally unstable* under the condition

$$\boxed{\frac{\rho_s h_s}{\rho_f \mu_{max}} < 1.}$$

Hence, the scheme becomes unstable if the density of the structure becomes too small with respect to the density of the fluid or if the maximum eigenvalue of the added mass operator (which depends on its turn on the aspect ration of the domain) becomes too large. This is in perfect agreement with our previous numerical observations (see e.g. [2]).

We consider also the implicit version of (4), obtained by getting implicit the discretization of the structure equation. In this case it can be easily shown that the resulting fluid-structure scheme is unconditionally stable. Yet, at each time step we have to solve a non-linear system. For its solution we first consider a Dirichlet/Neumann subiteration strategy: given an initial guess η_0 of the structure displacement, for each $k = 0, 1, \ldots$, we solve the fluid equations with imposed velocity on the interface and get a solution $(\mathbf{u}_k, p_k)$, we solve the structure and get $\tilde{\eta}_{k+1}$, we relax the new solution $\eta_{k+1} = \omega\tilde{\eta}_{k+1} + (1-\omega)\eta_k$ and we iterate until the difference between η_{k+1} and η_k is small enough.

This algorithm converges only if the relaxation parameter ω is taken small enough (see [3])

$$\boxed{0 < \omega < \frac{2(\rho_s h_s + a\delta t^2)}{\rho_s h_s + \rho_f \mu_{max} + a\delta t^2}.}$$

This result, not surprisingly, tells us that for those values for which the explicit algorithm is unstable, the implicit one need a relaxation parameter strictly smaller than 1 to converge.

A similar analysis can be carried out for the dual approach (Neumann/Dirichlet subiteration strategy) in which we solve the fluid equations with imposed pressure and we compute the unbalanced force on the structure by evaluating the residual of the structure equation. Details are given in [3].

Conclusions. The simple linear model (1) reproduces the instabilities observed on more complex non-linear problems. In our opinion, this is a clear indication that the source of such instabilities has to be sought in the incompressibility constraint of the fluid. Moreover, model (1) could be used as a tool to quickly check the stability/convergence of other partitioned algorithms.

Concerning applications in hemodynamics, with physiological values of the parameters, implicit fluid-structure algorithms should be used. Current research is directed to find efficient strategies to solve the fully coupled fluid-structure problem appearing at each time-step. Among others we mention exact Newton or quasi-Newton algorithms ([1, 6]) or non-linear domain decomposition strategies combined with Aitken extrapolation ([5]). Alternatively, one could consider *semi-implicit* partitioned algorithms in which the structure displacement is treated explicitly while the structure velocity is taken implicitly and coupled with the fluid equations. An example of a stable algorithm of this type is given in [2].

References

[1] J.F. Gerbeau and M. Vidrascu. A Quasi-Newton algorithm based on a reduced model for fluid-structure interactions problems in blood flows. *Math. Model. Num. Anal.*, 37(4):631–648, 2003.

[2] F. Nobile. *Numerical approximation of fluid-structure interaction problems with application to haemodynamics*. PhD thesis, EPFL, Switzerland, 2001.

[3] P. Causin and J.F. Gerbeau and F. Nobile. Added-mass effect in the design of partitioned algorithms for fluid-structure problems. *Comp. Meth. Appl. Mech. Engrg.*, in press.

[4] A.Quarteroni and L. Formaggia. Mathematical Modelling and Numerical Simulation of the Cardiovascular System. Chapter in *Modelling of Living Systems, Handbook of Numerical Analysis Series*, P.G Ciarlet et J.L. Lions Eds., Elsevier, Amsterdam, 2003.

[5] S. Deparis and M. Discacciati and A. Quarteroni A domain decomposition framework for fluid-structure interaction problems. Report MOX 45, 2004.

[6] M.A. Fernández and M. Moubachir. A Newton method using exact jacobians for solving fluid-structure coupling. *Computers & Structures,* vol. 83, num. 2-3, pp. 127-142, 2005.

Numerical simulation of viscoelastic flows with complex surfaces in 3D

Marco Picasso

(joint work with Andrea Bonito, Philippe Clément)

A numerical model is presented for the simulation of viscoelastic flows with complex free surfaces in three space dimensions. The mathematical formulation of the model is similar to that of the volume of fluid method, but the numerical procedures are different.

Following [1, 2, 3], a splitting method is used for the time discretization. The prediction step consists in solving three advection problems, one for the volume fraction of liquid, one for the velocity field, one for the extra-stress. The correction step corresponds to solving an Oldroyd-B fluid flow problem without advection.

Two different grids are used for the space discretization. The three advection problems are solved on a fixed, structured grid made out of small cubic cells, using a forward Characteristics method. The Oldroyd-B problem without advection is solved using continuous, piecewise linear stabilized finite elements on a fixed, unstructured mesh of tetrahedra.

Efficient post-processing algorithms enhance the quality of the numerical solution. A hierarchical data structure reduces the memory requirements.

Numerical results are presented for the stretching of a filament. Fingering instabilities are obtained when the aspect ratio is large. Also, results pertaining to jet buckling are reported.

Finally, a time dependent Oldroyd-B fluid flow problem without advection is considered. As in [4] an implicit function theorem is used to prove existence of a solution and convergence of the finite element method. A maximum regularity property for the three-fields Stokes problem in $L^q(L^r)$ spaces is used to prove existence.

References

[1] V. Maronnier, M. Picasso and J. Rappaz, *Numerical simulation of free surface flows*, J. Comp. Phys. **155** (1999), 439–455.

[2] V. Maronnier, M. Picasso and J. Rappaz, *Numerical simulation of three-dimensional free surface flows*, Internat. J. Numer. Methods Fluids. **42** (2003), 697–716.

[3] A. Caboussat, M. Picasso and J. Rappaz, *Numerical simulation of free surface incompressible liquid flows surrounded by compressible gas*, J. Comp. Phys., **203** (2005), 626–649.

[4] M. Picasso, J. Rappaz, *Existence, a priori and a posteriori error estimates for a nonlinear three field problem arising from Oldroyd-B viscoelastic flows*, Math. Model. Numer. Anal., **35** (2001), 879–897.

Adaptive finite elements with high aspect ratio for the computation of dendritic growth with convection

Marco Picasso

(joint work with Jacek Narski)

A solutal phase-field model for dendritic growth of an isothermal binary alloy is considered. The liquid flow due to different solid and liquid densities is also taken into account. The model then corresponds to coupling the phase-field equation, the concentration equation and the compressible Navier-Stokes equations in the liquid.

Following [1, 2, 3] an adaptive finite element method is used. The goal of the adaptive algorithm is to produce a sequence of triangulations such that the relative estimated error is close to a preset tolerance. Moreover, the error estimator allows the triangles to have large aspect ratios whenever needed. The algorithm is justified in [2] when convection in the liquid is absent.

Numerical results are reported for the hot tearing experiment. Negative pressures are obtained, predicting the onset of microporosity.

References

[1] M. Picasso, *An anisotropic error indicator based on Zienkiewicz-Zhu error estimator : application to elliptic and parabolic problems*, SIAM J. Sci. Comp. **24** (2003), 1328–1355.

[2] E. Burman, M. Picasso, *Anisotropic, adaptive finite elements for the computation of a solutal dendrite, J. Interfaces and Free Boundaries*, **5** (2003), 103–127.

[3] E. Burman, A. Jacot, M. Picasso, *Adaptive finite elements with high aspect ratio for the computation of coalescence using a phase-field model*, J. Comp. Phys. **195** (2004), 153–174.

A Finite Element based Level Set Method for Two-Phase Incompressible Flows

Arnold Reusken

We consider a domain $\Omega \subset \mathbb{R}^3$ which contains two different immiscible incompressible newtonian phases (fluid-fluid or fluid-gas). The model problem is a liquid drop contained in a surrounding fluid. The time-dependent domains which contain the phases are denoted by $\Omega_1 = \Omega_1(t)$ and $\Omega_2 = \Omega_2(t)$ with $\overline{\Omega}_1 \cup \overline{\Omega}_2 = \overline{\Omega}$. We assume $\partial\Omega_1 \cap \partial\Omega = \emptyset$. The interface between the two phases ($\partial\Omega_1 \cap \partial\Omega_2$) is denoted by $\Gamma = \Gamma(t)$. To model the forces at the interface we make the standard assumption that the surface tension balances the jump of the normal stress on the interface, i.e., we have a free boundary condition

$$[\boldsymbol{\sigma}\mathbf{n}]_\Gamma = \tau\kappa\mathbf{n} \ ,$$

with $\mathbf{n} = \mathbf{n}_\Gamma$ the unit normal at the interface (pointing from Ω_1 in Ω_2), τ the surface tension coefficient (material parameter), κ the curvature of Γ and $\boldsymbol{\sigma}$ the stress tensor

$$\boldsymbol{\sigma} = -p\mathbf{I} + \mu\mathbf{D}(\mathbf{u}), \quad \mathbf{D}(\mathbf{u}) = \nabla\mathbf{u} + (\nabla\mathbf{u})^T \ ,$$

with $p = p(x,t)$ the pressure, $\mathbf{u} = \mathbf{u}(x,t)$ the velocity vector and μ the viscosity. We assume continuity of the velocity across the interface. In combination with the conservation laws of mass and momentum this yields the following standard model:

$$\begin{cases} \rho_i\big(\frac{\partial\mathbf{u}}{\partial t} + (\mathbf{u}\cdot\nabla)\mathbf{u}\big) = -\nabla p + \rho_i\mathbf{g} + \operatorname{div}(\mu_i\mathbf{D}(\mathbf{u})) & \text{in } \Omega_i \\ \operatorname{div}\mathbf{u} = 0 & \text{in } \Omega_i \end{cases} \quad \text{for } i = 1,2$$

$$[\boldsymbol{\sigma}\mathbf{n}]_\Gamma = \tau\kappa\mathbf{n}, \quad [\mathbf{u}\cdot\mathbf{n}]_\Gamma = 0 \ .$$

The vector $\mathbf{g}$ is a known external force (gravity). In addition we need initial conditions for $\mathbf{u}(x,0)$ and boundary conditions at $\partial\Omega$. For simplicity we assume homogeneous Dirichlet boundary conditions.

This model for a two-phase incompressible flow problem is often used in the literature. The effect of the surface tension can be expressed in terms of a localized force at the interface, cf. the so-called continuum surface force (CSF) model [7, 9]. This localized force is given by

$$f_\Gamma = \tau\kappa\delta_\Gamma\mathbf{n}_\Gamma \ .$$

Here δ_Γ is a Dirac δ-function with support on Γ. This localization approach can be combined with the level set method for capturing the unknown interface. Combination of the CSF approach with the level set method leads to the following model for the two-phase problem in $\Omega \times [0,T]$

$$\rho(\phi)\Big(\frac{\partial\mathbf{u}}{\partial t} + (\mathbf{u}\cdot\nabla)\mathbf{u}\Big) = -\nabla p + \rho(\phi)\mathbf{g} + \operatorname{div}(\mu(\phi)\mathbf{D}(\mathbf{u})) + \tau\kappa\delta_\Gamma\mathbf{n}_\Gamma \tag{1}$$

$$\operatorname{div}\mathbf{u} = 0 \tag{2}$$

$$\phi_t + \mathbf{u}\cdot\nabla\phi = 0 \tag{3}$$

together with suitable initial and boundary conditions for $\mathbf{u}$ and ϕ. This is the continuous problem that we use to model our two-phase problem. It is also used in, for example, [9, 14, 15, 17, 18, 19, 20].

In this talk we present an overview of an method that has been developed and implemented in the DROPS package for the efficient numerical simulation of this model. The main characteristics of the method are the following:

- For capturing the interface between the two phases the level set method is applied [9, 14, 13].
- The spatial discretization is based on a hierarchy of tetrahedral grids. These grids are constructed in such a way that they are consistent (no hanging nodes) and that the hierarchy of triangulations is stable. The main ideas are taken from [5, 6, 3, 4, 12]. An important property is that local refinement and coarsening are easy to realize.
- For discretization of velocity, pressure and the level set function we use conforming finite elements. An example (used in the numerical experiments) is the Hood-Taylor $P_2 - P_1$ finite element pair for velocity and pressure and piecewise quadratic P_2 finite elements for the level set function.
- For the time discretization we apply a variant of the fractional step θ-scheme, due to [8].
- In each time step discrete Stokes problems and a discrete nonlinear elliptic system for the velocity unknowns must be solved. For the former we use an inexact Uzawa method with a suitable multigrid preconditioner. The latter problems are solved by a Picard iteration combined with a Krylov subspace method.
- For numerical and algorithmic purposes it is advantageous to keep the level set function close to a signed distance function during the time evolution. To realize this a reparametrization technique is needed. We apply a variant of the Fast Marching method [11, 16].

The above list can be extended by two model-specific points:

- The effect of surface tension is modeled by using the above-mentioned continuum surface force technique [7, 9].
- For the treatment of the localized force term we apply a technique based on a partial integration rule for the Laplace-Beltrami operator, cf. [1, 2, 10]. Due to this approach the second order derivatives coming from the curvature can be eliminated.

We discuss certain aspects of our solver in more detail. Results of numerical experiments for a three dimensional instationary two-phase fluid-fluid flow problem are presented.

References

[1] E. Bänsch, *Numerical methods for the instationary Navier-Stokes equations with a free capillary surface*, Habilitation thesis (1998) Albert-Ludwigs-University Freiburg.

[2] E. Bänsch, *Finite element discretization of the Navier-Stokes equations with a free capillary surface*, Numer. Math. **88** (2001), 203–235.

[3] P. Bastian, *Parallele adaptive Mehrgitterverfahren* (1996) Teubner, Stuttgart.
[4] P. Bastian, K. Birken, K. Johannsen, S. Lang, N. Neuß, H. Rentz-Reichert, C. Wieners, *UG - A flexible software toolbox for solving partial differential equations*, Computing and Visualization in Science **1** (1997), 27–40.
[5] J. Bey, *Finite-Volumen- und Mehrgitterverfahren für elliptische Randwertprobleme*, Advances in Numerical Methods (1998), Teubner, Stuttgart.
[6] J. Bey, *Simplicial grid refinement: on Freudenthal's algorithm and the optimal number of congruence classes*, Numer. Math. **85** (2000), 1–29.
[7] J. U. Brackbill, D. B. Kothe, C. Zemach, *A continuum method for modeling surface tension*, J. Comput. Phys. **100** (1992), 335–354.
[8] M. O. Bristeau, R. Glowinski, J. Periaux, *Numerical methods for the Navier-Stokes equations. Application to the simulation of compressible and incompressible flows*, Computer Physics Report **6** (1987), 73–188.
[9] Y. C. Chang, T. Y. Hou, B. Merriman, S. Osher, *A level set formulation of Eulerian interface capturing methods for incompressible fluid flows*, J. Comput. Phys.
textbf24 (1996), 449–464.
[10] G. Dziuk, *An algorithm for evolutionary surfaces*, Numer. Math. **58** (1991), 603–611.
[11] R. Kimmel, J. A. Sethian, *Computing geodesic paths on manifolds*, Proc. Natl. Acad. Sci. **95** (1998), 8431–8435.
[12] S. Lang, *Parallele numerische Simulation instationärer Probleme mit adaptiven Methoden auf unstrukturierten Gittern*, Ph.D. thesis (2001), University of Stuttgart.
[13] S. Osher, J. A. Sethian, *Fronts propagating with curvature dependent speed: algorithms based on Hamilton-Jacobi formulations*, J. Comp. Phys. **79** (1988), 12–49.
[14] S. Osher, R. P. Fedkiw, *Level set methods: An overview and some recent results*, J. Comput. Phys. **169** (2001), 463–502.
[15] S. B. Pillapakkam, P. Singh, *A level-set method for computing solutions to viscoelastic two-phase flow*, J. Comput. Phys. **174** (2001), 552–578.
[16] J. A. Sethian, *A fast marching level set method for monotonically advancing fronts*, Proc. Natl. Acad. Sci. **93** (1996), 1591–1597.
[17] M. Sussman, P. Smereka, S. Osher, *A level set approach for computing solutions to incompressible two-phase flow*, J. Comp. Phys. **114** (1994), 146–159.
[18] M. Sussman, A. S. Almgren, J. B. Bell, Ph. Colella, L. H. Howell, M. L. Welcome, *An adaptive level set approach for incompressible two-phase flows*, J. Comp. Phys. **148** (1999), 81–124.
[19] A.-K. Tornberg, *Interface tracking methods with application to multiphase flows*, Doctoral Thesis (2000), Royal Institute of Technology, Department of Numerical Analysis and Computing Science, Stockholm.
[20] A.-K. Tornberg, B. Engquist, *A finite element based level-set method for multiphase flow applications*, Comput. Visual. Sci. **3** (2000), 93–101.

Direct Simulation of the Motion of Particles in Viscous Flows

Stefan Turek
(joint work with Decheng Wan)

The motion of particles in an incompressible viscous fluid is widely found in various processes such as foods containing particles, fluidization of catalyst beds, separation process using cyclones, sedimentation, just to name a few. Direct numerical simulation of the motion of particles in laminar fluids is a very challenging

task. The particles are moved by Newton's laws under the action of hydrodynamic forces computed from the numerical solution of the incompressible Navier-Stokes equations. On the other hand, the fluid field and domain are disturbed and changed simultaneously due to the motion of particles. It is crucial that in the practical cases in which there are often large number particles (greater than 10,000) existing in fluids, the complex interaction between fluid and particles as well as the collision between particles is a challenging task for any numerical scheme.

So far, such problems have motivated the development of numerous algorithms, which can be broadly classified into two families. The first is a generalized ALE standard Galerkin finite element method [1, 2] in which both the fluid and particle equations of motion are incorporated into a single coupled variational equation. The hydrodynamic forces and torques on the particles are eliminated in the formulation. The computation is performed on an unstructured body-fitted grid, and an arbitrary Lagrangian-Eulerian (ALE) moving mesh technique is adopted to deal with the motion of the particles. In this scheme, the positions of the particles and grid nodes are updated explicitly, while the velocities of the fluid and the solid particles are determined implicitly. The second approach is based on the principle of embedded or fictitious domains. Glowinski, Joseph and coauthors [3] developed a distributed Lagrange multiplier (DLM)/fictitious domain method. In the DLM method, the entire fluid-particle domain is assumed to be a fluid and then to constrain the particle domain to move with a rigid motion. The fluid-particle motion is treated implicitly using a combined weak formulation in which the mutual forces cancel. The DLM method is referred to as an implicit fictitious boundary approach since there is no need to directly calculate the hydrodynamic forces exerted on the particles. The obvious advantage of the implicit fictitious boundary approach is that the computational time for the calculation of forces exerted on particles can be saved. However, the implicit coupling of fluid-solid momentum equations slows down the solution procedure, since it requires the solution of large systems of the linear and nonlinear algebraic equations for the coupled variables of fluid and solid.

In [5, 6], we proposed a multigrid FEM-based explicit fictitious boundary method (FBM). In contrast to the implicit fictitious domain approach, the explicit fictitious boundary approach is to solve fluid equations and solid equations separately. The main point is that the forces exerted on particles can be calculated in a very efficient way. The computational cost are practically independent of the number of particles in the computational domain. The FBM is based on an unstructured FEM background grid. The flow is computed by a multigrid finite element solver and the solid particles are allowed to move freely through the computational mesh which can be chosen independently from the particles of arbitrary shape, size and number. The same fixed grid is also used to represent the location of the solid particles by imposing the velocities on the nodes covered by the particles at any time. The new positions and the new velocities of the particles are updated using Newton's law so that there is no need to remesh the domain. The interaction between the fluid and the particles is taken into account by the FBM in which an explicit volume based calculation for the hydrodynamic forces is integrated. Based

on the boundary conditions applied at the interface between the particles and the fluid which can be seen as an additional constraint to the governing Navier-Stokes equations, the fluid domain can be extended into the whole domain which covers both fluid and particle domains. It starts with a coarse mesh which may contain already many of the geometrical fine-scale details, and employs a (rough) boundary parametrization which sufficiently describes all large-scale structures with regard to the boundary conditions. Then, all fine-scale features are treated as interior objects such that the corresponding components in all matrices and vectors are unknown degrees of freedom which are implicitly incorporated into all iterative solution steps. For treating more than one particle, a collision model is needed to prevent particles from interpenetrating each other. Collisions or near-collisions between the particles present severe difficulties in direct simulations of particulate flows. Even near-collisions can greatly increase the cost of a simulation, because in order to simulate the particle-particle interaction mechanism in a direct manner, the flow fields in the narrow gap between the converging particle surfaces must be accurately resolved. For solving the problem, we describe a new repulsive force model which cannot only handle to prevent the particles from getting too close to each other, it can also deal with the case of particle overlapping when numerical simulations bring the particles very close or even overlapping due to unavoidable numerical trunaction error.

We present several cases of simulations as proposed benchmark configurations to evaluate and to validate the accuracy and efficiency of the presented method by a careful comparison between the results obtained by the presented method and a standard body-fitted computation for two-dimensional flow around a circular body in a channel. Flow with one rotating and moving particle is shown to validate the calculations of angular velocity and translational velocities by the presented multigrid FBM. The cases with two and many particles are given to check the quality of the collision model and of the efficiency of the multigrid FBM for the simulation of particulate flow with large numbers of particles. We also adopt the multigrid FEM fictitious boundary method to simulate solid-liquid two phase flows with huge number of moving particles in fluid. As an illustration, numerical results of three big disks plunging into 2000 small particles, and sedimentation of 10,000 particles in a cavity are presented.

The main advantage of the multigrid FBM is that the solid particles, which are allowed to have different shape and size, can move freely through the computational mesh for the fluid part which has not to change in time. The accuracy for capturing the particles is only of first order which is important for the explicit calculation of the correct fluid forces acting on the particles, however, it can be improved via special 'grid deformation' techniques to reach a local alignment with the particle surfaces. The proposed volume-based integration for the calculations of the hydrodynamic forces acting on the moving particles is one of the key ingredients of the multigrid FBM, and its high accuracy has been proven by numerous comparisons between the presented results and corresponding reference results from own computations or from literature: This new approach can be easily

incorporated into (almost) all CFD codes without the need for additional (background) meshes for the particles or special interpolation procedures since it only requires changes in the treatment of Dirichlet boundary conditions. The comparison with more implicit scheme, for instance [3], is not yet clear, particularly with respect to the total efficiency: Hence, it is absolutely necessary to design approximate benchmarks for realistic particulate flows. Another advantage of this new approach is that very different shapes and sizes of particles can be easily included; even coalesence and breakup mechanisms are possible.

The newly modified collision model based on the models by Joseph, Glowinski et al. [3, 4] with a new definition of a short range repulsive force cannot only prevent the particles from getting too close to each other, it can also deal with the case of overlapping when the numerical simulation brings the particles very close or even leads to overlapping. Special data structures and time reducing techniques for handling the calculation of large number of particles are described to enable the multigrid FBM to efficiently solve for many particles. Therefore, one of the next aims is to simulate in 2D up to 10^6 particles on a single PC/workstation while the corresponding 3D module in FeatFlow will be based on a parallel implementation for such a high number of particles. Furthermore, non-Newtonian and viscoelastic fluids (see [3]) have to be tackled in future.

References

[1] H.H. Hu, D.D. Joseph, and M.J. Crochet, *Direct simulation of fluid particle motions*, Theor. Comp. Fluid Dyn. **3** (1992), 285–306.

[2] B. Maury, *Direct Simulations of 2D fluid-particle flows in biperiodic domains*, J. Comput. Phy. **156** (1999), 325–351.

[3] R. Glowinski, T.W. Pan, T.I. Hesla, D.D. Joseph and J. Periaux, *A fictitious domain approach to the direct numerical simulation of incompressible viscous flow past moving rigid bodies: Application to particulate flow*, J. Comput. Phy. **169** (2001), 363–426.

[4] P. Singh, T.I. Hesla and D.D. Joseph, *Distributed Lagrange multiplier method for particulate flows with collisions*, Int. J. Multiphase Flow **29** (2003), 495–509.

[5] D.C. Wan, S. Turek and L.S. Rivkind, *An efficient multigrid FEM solution technique for incompressible flow with moving rigid bodies*, Numerical Mathematics and Advanced Applications, ENUMATH 2003, Springer (2004), 844–853.

[6] D.C. Wan, and S. Turek, *Direct numerical simulation of particulate flow via multigrid FEM techniques and the fictitious boundary method*, preprint version, University of Dortmund, (2004).

Phase Field/Level Set Methods for Problems Involving Elasticity

Noel J. Walkington

1. Overview

Models of physical systems often contain implicitly defined surfaces separating different phases, materials, etc. which may evolve over time. Phase field and level set techniques can be used to represent such interfaces without explicitly parameterizing them. When the evolution of the free surfaces can be determined from

"Eulerian" quantities (such as the curvature, flow velocity, etc.) phase field/level set representations have lead to very general robust algorithms and numerical codes to simulate these complex physical systems. This work considers how such algorithms may be extended to model free surfaces, such as elastic membranes, whose evolution depends additionally upon "Lagrangian" quantities, e.g. strain.

Currently there are no results on the existence and uniqueness for systems of partial differential equations modeling flows transporting elastic components, so analysis of algorithms to simulate these systems is not possible. However, results are available for the simpler system modeling the flow of two immiscible, incompressible Newtonian fluids, and convergence of numerical schemes for this problem are considered.

2. Flow of Immiscible Fluids

The simplest example of a multicomponent flow is the motion of two immiscible, incompressible Newtonian fluids. To model this problem it is convenient to introduce a "phase function" ϕ such that

$$\phi(x,t) = \begin{cases} +1/2 & \text{in fluid (1)} \\ -1/2 & \text{in fluid (2)} \end{cases}$$

The equations of motion in a domain $\Omega \subset \mathbb{R}^d$ can then be written as

$$\int_\Omega \rho(\phi)\left(v_t + (v.\nabla)v\right).w - p\,div(w) + \mu(\phi)D(v)\cdot D(w) = \int_\Omega \rho(\phi) f.w,$$

$$div(v) = 0, \qquad \phi_t + v.\nabla\phi = 0.$$

Here $D(v) = (1/2)(\nabla v + (\nabla v)^T)$ is the symmetric part of the velocity gradient, and the momentum equation is written in weak form to avoid explicit statement of the force balance across the interface(s) between the fluids. The density ρ and viscosity μ may take different values in each fluid:

$$\rho(\phi) = (1/2+\phi)\rho_1 + (1/2-\phi)\rho_2, \qquad \mu(\phi) = (1/2+\phi)\mu_1 + (1/2-\phi)\mu_2.$$

Convergence of numerical approximations to this system of equations has been established by the author. The key step is to develop a discrete version [3] of the DiPerna Lions theory [1] for the convection equation satisfied by ϕ.

3. Flows Containing Membranes

The stresses in a membrane $S(t)$ depend upon the deformation from a reference configuration $S_r \subset \Omega_r$. The deformation is usually expressed using differential geometry; however, for membranes transported in a fluid their deformation is inherited from the global deformation $\chi : \Omega_r \times [0,T] \to \Omega$ of the fluid; that is, $S(t) = \chi(S_r, t)$.

If $x = \chi(X,t)$, the deformation of the gradient of the fluid is $F = [\partial x_i/\partial X_\alpha]$, and

$$\int_\Omega (\ldots)dx = \int_{\Omega_r} (\ldots) J\,dX \qquad \text{where } J = det(F).$$

An application of the chain rule shows that $F = F(x,t)$ evolves according to $F_t + (v.\nabla)F = (\nabla v)F$.

3.1. **Membrane Kinematics.** If $\chi_s = \chi|_{S_r}$, then $d\chi_s : TS_r \to TS(t)$ is a linear map, so there exists a unique 3×3 matrix F_s of rank 2 such that

$$d\chi_s w = F_s w, \qquad w \in TS_r.$$

A calculation shows that $F_s = F(I - N \otimes N)$, where $N = N(X)$ is the normal to S_r. The matrix F_s carries the first fundamental form of the surface; in particular,

$$\int_{S(t)} (\ldots) da = \int_{S_r} (\ldots) J_s \, dA \qquad \text{where } J_s = \iota_2(F_s^T F_s)^{1/2}.$$

Here $\iota_2(F_s^T F_s)$ is the second invariant of the matrix $F_s^T F_s$ (since F_s has rank 2, this is the product of the two non-zero eigenvalues of $F_s^T F_s$).

3.2. **Sharp interface Equations.** If the membrane is hyperelastic, then the stresses are determined from a strain energy function $W : \mathbb{R}^{3\times 3} \to \mathbb{R}$. The equations governing the motion hyperelastic membranes separating two incompressible Newtonian fluids are then

$$\int_\Omega \rho(\phi)\dot{v}.w - p\, div(w) + \mu(\phi)D(v)\cdot D(w) + \int_{S(t)} (1/J_s)DW(F_s)\cdot(\nabla w)F_s = \int_\Omega \rho(\phi) f.w,$$

$$div(v) = 0 \qquad \phi_t + v.\nabla\phi = 0,$$

$$F_{st} + (v.\nabla)F_s = (\nabla v)F_s \qquad \text{on } S(t).$$

The interface $S(t)$ is implicitly defined as the jump set of ϕ.

A formal calculation shows that this system satisfies the classical energy estimate,

$$\frac{d}{dt}\left(\int_\Omega (\rho(\phi)/2)|v|^2 + \int_{S_r} W(F_s)\right) + \int_\Omega \mu(\phi)|D(v)|^2 = \int_\Omega \rho(\phi) f.v.$$

3.3. **Phase Field Approximations.** The surface $S(t)$ is implicitly defined to be the jump set of ϕ. If ϕ has bounded variation then

$$\int_{S(t)} (\ldots) da = \int_\Omega (\ldots)|\nabla\phi| dx;$$

that is, surface measure da is $|\nabla\phi|dx$. For elastic membranes surface area in the reference configuration may be calculated as

$$\int_{S_r} (\ldots) dA = \int_{S(t)} (\ldots)(1/J_s) da = \int_\Omega (\ldots)(1/J)|F^T\nabla\phi| dx.$$

Phase field approximations introduce a smooth approximation of ϕ which rapidly changes from $-1/2$ to $+1/2$ across $S(t)$. If $\delta = (1/J)|F^T\nabla\phi|$ then

$$\delta_t + (v.\nabla)\delta + div(v)\delta = 0.$$

The phase field approximation of the flow of two fluids separated by an elastic membrane is then

$$\int_\Omega \rho(\phi)\dot{v}.w - p\,div(w) + \mu(\phi)D(v)\cdot D(w) + DW(F_s)\cdot(\nabla w)F_s\delta = \int_\Omega \rho(\phi)f.w,$$

$$div(v) = 0, \qquad \phi_t + v.\nabla\phi = 0,$$

$$F_{st} + (v.\nabla)F_s = (\nabla v)F_s, \qquad \delta_t + (v.\nabla)\delta = 0.$$

If reference configuration is taken to be the initial state, and if the membrane is initially stress free, then the initial data for F_s and δ can be determined from the initial value ϕ_0 of ϕ as $F_s = (I - N\otimes N)$, and $\delta = |\nabla\phi_0|$, where $N = \nabla\phi_0/|\nabla\phi_0|$.

The equations discussed above present many mathematical challenges; for example

- The regularity of the velocity is guaranteed by the energy estimate is $v \in L^\infty[0,T;L^2(\Omega)] \cap L^2[0,T;H^1(\Omega)]$. If a surface is transported by such a velocity field it is not clear that it remains sufficiently regular to define surface measure etc.
- The system contain the equations of nonlinear elasticity and currently there is no satisfactory existence and uniqueness theory for these equations.

  Frequently the membrane is significantly stiffer than the fluid and in this situation it is possible to develop a small strain theory for the above system of equations using the ideas developed in [2]. While this eliminates some problems others remain.

References

[1] R. J. DiPerna and P. L. Lions, *Ordinary differential equations, transport theory and Sobolev spaces*, Inventiones Mathematicae, *98* (1989), 511–547.

[2] Liu, Chun, Walkington, Noel J., *An Eulerian description of fluids containing visco-elastic particles*, Arch. Ration. Mech. Anal., *159*, No. 3, (2001), 229-252.

[3] N. J. Walkington, *Convergence of the discontinuous Galerkin method for discontinuous solutions*, SIAM Journal on Numerical Analysis, *42* No. 5, (2005).

Reporter: Noel J. Walkington

Participants

Prof. Dr. Eberhard Bänsch

Institut f. Angew. Mathematik III
Universität Erlangen
Haberstr. 2
91058 Erlangen

Prof. Ph.D. Marek Behr

Chair of Computational Analysis of
Technical Systems (CATS)
Cen.for Computational Eng.Science
RWTH Aachen University
52056 Aachen

Dr. Erik Burman

Institut d'Analyse et Calcul
Scientifique, Fac. des Sc. de Base
EPFL Lausanne
SB-IACS-ASN, Bat.MA, Station 8
CH-1015 Lausanne

Sashikumaar Ganesan

Institut für Analysis und Numerik
Otto-von-Guericke-Universität
Magdeburg
Postfach 4120
39016 Magdeburg

Prof. Dr. Lucia Gastaldi

Dipartimento di Matematica
Universita di Brescia
Via Valotti 9
I-25133 Brescia

Dr. Yon Chol Kim

Institute of Mathematics
Gang Myong Dong, Un Jong District
Pyong Yang City
D.P.R. of Korea

Dr. Petr Knobloch

Department of Computational Math.
Faculty of Mathematics and Physics
Charles University Prague
Sokolovska 83
186 75 Prague 8
Czech Republic

Rolf Krahl

Institut f. Angew. Mathematik III
Universität Erlangen
Haberstr. 2
91058 Erlangen

Dr. Gunar Matthies

Fakultät für Mathematik
Ruhr-Universität Bochum
44780 Bochum

Jürgen Mehnert

Institut für Angewandte Mathematik
Universität Freiburg
Hermann-Herder-Str. 10
79104 Freiburg

Dr. Fabio Nobile

Dipartimento di Matematica
Politecnico di Milano
Via Bonardi 9
I-20133 Milano

Dr. Marco Picasso

Institut d'Analyse et Calcul
Scientifique, Fac. des Sc. de Base
EPFL Lausanne
SB-IACS-ASN, Bat.MA, Station 8
CH-1015 Lausanne

Prof. Dr. Arnold Reusken

Institut für Geometrie und
Praktische Mathematik
RWTH Aachen
Templergraben 55
52062 Aachen

Prof. Dr. Lutz Tobiska

Institut für Analysis und Numerik
Otto-von-Guericke-Universität
Magdeburg
Postfach 4120
39016 Magdeburg

Dr. Stefan Turek

Institut für Angewandte Mathematik
Universität Dortmund
Vogelpothsweg 87
44227 Dortmund

Prof. Dr. Noel J. Walkington

Department of Mathematical Sciences
Carnegie Mellon University
Pittsburgh, PA 15213-3890
USA